Musajo, L., & Rodighiero, G. (1972) in *Photophysiology* (Giese, A. C., Ed.) Vol. VII, pp 115–147, Academic Press, New York.
Musajo, L., Rodighiero, G., Breccia, A., Dall'Acqua, F., & Malesani, G. (1966) *Photochem. Photobiol. 7*, 739–745.
Muto, A., Ehresmann, C., Fellner, P., & Zimmermann, R. A. (1974) *J. Mol. Biol. 86*, 411–432.
Nomura, M., Traub, P., & Bechmann, H. (1968) *Nature (London) 219*, 793–799.
Ou, C.-N., & Song, P.-S. (1978) *Biochemistry 17*, 1054–1059.
Reiner, A. M. (1969) *J. Bacteriol. 97*, 1431–1436.
Rich, A., & RajBhandary, U. L. (1976) *Annu. Rev. Biochem. 45*, 805–860.
Rodighiero, G., Musaco, L., Dall'Acqua, F., Marciani, S., Caporale, G., & Ciavatta, L. (1970) *Biochim. Biophys. Acta 217*, 40–49.
Schulte, C., Morrison, C. A., & Garrett, R. A. (1974) *Biochemistry 13*, 1032–1037.
Seals, A. A., & Champney, W. S. (1976) *Biochem. Biophys. Res. Commun. 72*, 753–760.
Shen, C.-K. J., & Hearst, J. E. (1976) *Proc. Natl. Acad. Sci. U.S.A. 73*, 2649–2653.
Sypherd, P. S. (1971) *J. Mol. Biol. 56*, 311–318.
Traub, P., & Nomura, M. (1969) *J. Mol. Biol. 40*, 391–413.
Traub, P., Mizushima, S., Lowry, C. V., & Nomura, M. (1971) *Methods Enzymol. 20*, 391–407.
Yoakum, G. H., & Cole, R. S. (1978) *Biochim. Biophys. Acta 521*, 529–546.
Zimmermann, R. A. (1974) in *Ribosomes* (Nomura, M., Tissieres, A., & Lengyel, P., Eds.) pp 225–269, Cold Spring Harbor Laboratory, Cold Spring Harbor, NY.

Conformation of *Escherichia coli* Ribosomal Protein L7/L12 in Solution: Hydrodynamic, Spectroscopic, and Conformation Prediction Studies†

Carl A. Luer and Kin-Ping Wong*

ABSTRACT: The conformation of *Escherichia coli* ribosomal protein L7/L12 in solution has been studied using spectroscopic and hydrodynamic methods. Circular dichroism studies in the near-ultraviolet region reveal two bands at 262 and 268 nm originating from the tertiary conformational environment of the phenylalanyl residues. Additional characterization of the phenylalanine environment includes an intrinsic fluorescence emission spectrum arising from the phenylalanine fluorophores. Computer analysis of the far-ultraviolet circular dichroism spectrum suggests that L7/L12 contains as much as ~76% α helix. Hydrodynamic properties of L7/L12, measured with the purpose of providing relevant shape information, include the frictional coefficient ratio (1.84 ± 0.03) and intrinsic viscosity (28 ± 0.4 mL/g). The experimentally determined frictional coefficient ($6.15 \pm 0.15 \times 10^{-8}$) has been compared with theoretical calculations of the same value employing two independent methods and assuming various dimensions for the L7/L12 dimer. Combining the experimental results from this work with those available from the literature, and using conformation predictive methods of Chou & Fasman [P. Y. Chou & G. D. Fasman (1974) *Biochemistry 13*, 211–222, 222–245] and of Maxfield & Scheraga (F. R. Maxfield & H. A. Scheraga (1976) *Biochemistry 15*, 5138–5153), several possible molecular models of the L7/L12 dimer have been constructed and critically examined. A model which is consistent with all of the available data is proposed.

The elucidation of the molecular mechanism of ribosome self-assembly is a monumental task. The molecular components that make up the prokaryotic 70S ribosome from *Escherichia coli* include some 55 proteins and three species of RNA, providing the potential for a tremendous variety of inter- and intramolecular interactions. A prerequisite to the successful investigation of ribosomal self-assembly, however, is an understanding of the detailed molecular structures of the component proteins and RNAs.

Proteins L7 and L12, from the 50S subunit of *E. coli* ribosomes, were the first ribosomal proteins to be completely sequenced (Terhorst et al., 1972a, 1973). It was found that the two sequences were identical except for the presence of an acetylated amino-terminal serine group on L7 (Terhorst et al., 1972b). For this reason, they are commonly referred to as a single protein termed L7/L12. Considerable information has accumulated in the literature concerning the functional importance of this ribosomal protein, indicating that the presence of L7/L12 is required for the ribosome to carry out the initiation, elongation, and termination steps of protein synthesis (for a review, see Möller, 1974). Structural information about L7/L12, then, is necessary for a better understanding not only of the process of ribosomal self-assembly, but also of its important functional roles.

Early attempts to analyze the secondary structure using circular dichroism reveal that L7/L12 contains substantial amounts of α helix, estimates varying from 45 to 60%. These estimates, however, are calculated from single wavelength information and are based upon comparisons with poly-(α-amino acids) (Möller et al., 1970; Dzionara, 1970; Boublik et al., 1973). In addition, some of these measurements were obtained under denaturing conditions (Dzionara, 1970). Detailed analyses of circular dichroism data as well as other spectroscopic properties of protein L7/L12 obtained under functionally relevant conditions are not yet available. Pre-

† From the Department of Biochemistry, University of Kansas Medical Center, Kansas City, Kansas 66103. *Received October 13, 1978; revised manuscript received February 5, 1979.* This investigation was supported by Research Grants GM 22962 and in part by HL 18905 from the National Institutes of Health, U.S. Public Health Service, Bethesda, MD.

* National Institutes of Health Career Development Awardee (GM 70628).

0006-2960/79/0418-2019$01.00/0

dictions of secondary structure for L7/L12 that appear in the literature are based entirely on the information available in the amino acid sequence and suggest α-helical content varying from 42 to 64% depending upon the method used (Ptitsyn et al., 1973; Wittmann-Liebold et al., 1977). No β structure is evident from either prediction.

In solution, L7/L12 is known to exist as a dimer (Möller et al., 1972; Wong & Paradies, 1974) possessing an extremely elongated shape (Wong & Paradies, 1974; Österberg et al., 1976). Probably due to the elongated shape, attempts to crystallize the dimer have been unsuccessful so that the exact secondary structure, as well as information on the tertiary and quaternary structure, remains elusive. Although the successful crystallization of L7/L12 was reported earlier (Liljas & Kurland, 1976), subsequent analysis has indicated that a spontaneously generated amino-terminal fragment of the protein and not the intact L7/L12 dimer was crystallized (Liljas et al., 1978). Moreover, structural information on the crystallized material is not yet available.

Recently, a molecular model for the L7/L12 dimer in solution has been proposed (Gudkov et al., 1977). The proposed structure is based upon the combined use of the stereochemical theory of the tertiary structure of globular proteins (Lim, 1974a,b) and of chemical and physical data which were unavailable at the time the model was published.

In this report, we present hydrodynamic and spectroscopic properties as well as secondary structural predictions for L7/L12. Additionally, we have incorporated the experimental data from this report and those available from the literature and propose a possible three-dimensional structure for the L7/L12 dimer. This molecular model of protein L7/L12 was presented as a poster at the 11th FEBS (Federation of European Biochemical Societies) Annual Meeting in Copenhagen, Aug 17, 1977, together with all the supportive data [Abstract A2-9 219 5]. The model presented here and the model of Gudkov et al. (1977) are discussed in light of the available experimental data.

Experimental Procedures

Buffers: TMA buffer, 10 mM Tris-HCl, 20 mM $MgCl_2$, 30 mM NH_4Cl, pH 7.6; buffer A, 10 mM $MgCl_2$, 40 mM KCl, 10 mM imidazole hydrochloride, 1 mM 2-mercaptoethanol, pH 7.4; extraction buffer, 1.0 M NH_4Cl, 20 mM $MgCl_2$, 10 mM imidazole hydrochloride, 1 mM 2-mercaptoethanol, pH 7.4; TMK_{50} buffer, 10 mM Tris-HCl, 20 mM $MgCl_2$, 50 mM KCl, pH 7.6.

Preparation of Ribosomes. Escherichia coli strain MRE 600 (RNase I$^-$) was purchased from Microbiological Research Establishment, Porton, England, and stored at −70 °C until needed. The 70S ribosomes were isolated according to the procedure of Traub et al. (1971) with slight modification. One hundred grams of cell paste was diluted to 400 mL with TMA buffer. The thawed cells were disrupted by a precooled French press operated at 9 to 12 × 10^3 psi. The cell debris was removed by two successive centrifugations at 30000*g* for 30 min. The ribosomes were sedimented at 105000*g* for 6 h, followed by resuspension in a minimum amount of TMA buffer. The suspension was clarified by centrifugation for 15 min at 30000*g*, and 10-mL aliquots were layered on 30-mL portions of 30% sucrose in TMA buffer. The ribosomes were repelleted at 105000*g* for 18 h. The clarification and 18-h centrifugation steps were repeated. All operations were carried out at 4 °C. The final pellets were resuspended in buffer A and stored at −70 °C.

Purification of Protein L7/L12. In preparation for the extraction of L7/L12, approximately 500 mg of ribosomes was thawed and diluted to 60 mL with buffer A. Following a clarification spin at 30000*g* for 20 min, ribosomes were pelleted at 195000*g* for 4 h and resuspended in approximately 15 mL of extraction buffer. After dialysis against the same buffer at 4 °C, ribosomes were diluted to a concentration of 4 mg/mL with extraction buffer and treated according to the procedures of Hamel et al. (1972) for the isolation of L7/L12.

Protein samples were further purified by elution through a carboxymethylcellulose (CM 52) column equilibrated with 10 mM ammonium acetate, pH 6.0, followed by dialysis against 50 mM NH_4HCO_3, pH 7.8, and lyophilization. The sample was then applied to a Sephadex G-100 column equilibrated with TMK_{50} buffer.

All hydrodynamic and spectroscopic measurements were obtained in TMK_{50} buffer unless otherwise stated. This buffer is similar to those routinely used in functional assays of ribosomal particles and is, therefore, considered to approximate "native" conditions.

Viscosity. Viscosity measurements were made using a Ubbelohde semimicro dilution viscometer equilibrated in a Cannon Model MI constant-temperature bath thermostated at 25 ± 0.01 °C. Flow time for protein solutions over that of solvent ranged from 8.56 to 17.37 s. Generally, 8 to 10 flow time measurements were made on each solution. The intrinsic viscosity, $[\eta]$, was obtained according to eq 1, where t and t_0

$$[\eta] = \lim_{c\to 0} \eta_{red} = \lim_{c\to 0}\left(\frac{t - t_0}{ct_0} + \frac{1 - \bar{v}\rho}{\rho}\right) \qquad (1)$$

are the flow times in seconds for solute and solvent, respectively, c is the concentration in g/mL, $\bar{v}$ is the partial specific volume of the protein, and ρ is the density of the solvent in g/mL. The reduced viscosity was plotted vs. concentration and $[\eta]$ was determined by extrapolating the reduced viscosity to infinite dilution using a least squares analysis. Calculations based on viscosity data include determinations of the Huggins constant (Huggins, 1942), β factor (Scheraga & Mandelkern, 1953), and viscosity increment (Simha, 1940).

Sedimentation Velocity. Frictional coefficients were measured in a Beckman Model E analytical ultracentrifuge equipped with schlieren optics. A 30-mm aluminum single sector centerpiece was used with an An-E rotor. Photographic plates were read on a Nikon Model 6C microcomparator.

Theoretical calculations of the frictional coefficients for the molecular models were performed by two independent methods. In one computation, an extension of the Stokes equation to include ellipsoids of revolution, as suggested by Perrin (1936), was used in the form shown in eq 2, where η

$$f = 6\pi\eta R_p \frac{(1 - b^2/a^2)^{1/2}}{(b/a)^{2/3} \ln \dfrac{1 + (1 - b^2/a^2)^{1/2}}{b/a}} \qquad (2)$$

is viscosity of the solvent, a is the major semiaxis, b is the minor semiaxis, and R_p is the radius of a sphere of equal volume. In terms of major and minor semiaxes, R_p can be rewritten as $(ab^2)^{1/3}$.

A second theoretical calculation of the frictional coefficient was performed according to the method of Bloomfield et al. (1967a,b), in which the model dimensions are approximated by a combination of monomeric spheres of known radii. The calculation is summarized in eq 3, where n is the number of

$$f_p = \frac{n}{\dfrac{1}{f_m} + \dfrac{1}{6\pi\eta n_l}\sum_{l=1}^{n}\sum_{s=1}^{n}\langle R_{ls}^{-1}\rangle} \qquad (3)$$

spheres, f_m is the frictional coefficient of the monomeric spherical subunits, η is the viscosity of the solvent and $\langle R_{ls}^{-1} \rangle$ is the average reciprocal distance between the centers of subunits l and s. A more recent improvement of Bloomfield's theory which is better suited to dumbbell shaped models (De La Torre & Bloomfield, 1977) was used to calculate the theoretical frictional coefficient when such a shape was considered.

Ultraviolet Absorption. Ultraviolet absorption spectra were obtained with a Cary 118 CX double beam recording spectrophotometer equipped with derivative mode.

Fluorescence Spectroscopy. The intrinsic fluorescence of protein L7/L12 was recorded using a Perkin-Elmer MPF-44A fluorescence spectrophotometer. The emission spectrum of the sample buffer, including the peak due to Raman scattering, was recorded at a scale expansion of 20 and subtracted from the protein emission spectrum using a differential corrected spectra unit. The protein sample was excited at 257 nm with an excitation slit width of 3 nm, while the emission spectrum was recorded from 200 to 400 nm by using an emission slit width of 1.5 nm. An emission spectrum of a solution of L-phenylalanine under identical buffer conditions was obtained in the same manner and used as a reference for comparative purposes.

Circular Dichroism. CD[1] measurements were obtained from a JASCO Model J-20 spectropolarimeter. The temperature of the sample cell was controlled by a water-jacketed aluminum cell holder with constant-temperature water circulated from a Lauda K-2/R water bath. The temperature of the sample was measured directly with a telethermometer, Model YSI 425C. The results were expressed in terms of mean residue weight ellipticity, $[\theta]_{MRW}$, according to the equation: $[\theta]_{MRW} = (\theta \times MRW)/(dc)$, where θ is observed ellipticity in degrees, MRW is the mean residue weight of L7/L12 which was calculated to be 102, d is cell path length in decimeters, and c is protein concentration in g/mL. The instrument was calibrated routinely with d-camphor-10-sulfonic acid according to Cassim & Yang (1969). During all measurements, the spectropolarimeter was continuously purged with pure nitrogen gas.

Computer Analysis. Analyses of secondary structural information contained in far-ultraviolet circular dichroism spectra were carried out by the method of Yang and coworkers (Chen et al., 1974) using a BMD073 computer program (Biomedical Computer Programs, University of California Press, 1973) and an IBM 270/145 computer. According to this procedure, observed spectra were compared with model spectra for α helix, β conformation, and unordered structure as generated from X-ray crystallographic information from known proteins rather than from synthetic polypeptides. By using a modification of a nonlinear least-squares analysis, a form-fitted curve of known secondary structural contribution was generated.

Polyacrylamide Gel Electrophoresis. Sodium dodecyl sulfate–polyacrylamide gel electrophoresis was performed according to Weber & Osborn (1969). Discontinuous gel electrophoresis was carried out by the method of Davis (1964). Proteins used as molecular weight markers were bovine serum albumin, ovalbumin, bovine carbonic anhydrase B, myoglobin, and lysozyme.

Conformation Prediction. The secondary structure for protein L7/L12 was predicted from the amino acid sequence according to the methods of Chou & Fasman (1974a,b) and Maxfield & Scheraga (1976). Application of the former method employed updated potentials for α-helix and β-sheet structures (Fasman et al., 1976) and for β turns (Chou & Fasman, 1977) based on X-ray structural data of 29 proteins.

[1] Abbreviation used: CD, circular dichroism.

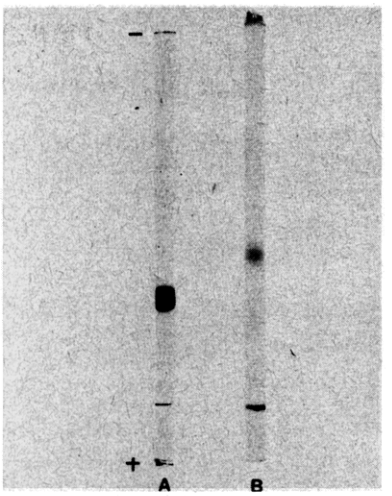

FIGURE 1: Polyacrylamide gel electrophoresis of *E. coli* ribosomal protein L7/L12. (A) Polyacrylamide (10%) gel in the presence of 0.1% sodium dodecyl sulfate. (B) Polyacrylamide (7.5%) gel at pH 8.9.

Miscellaneous. Ribosome concentrations were determined spectrophotometrically using $A_{260}^{1mg/mL}$ equal to 14.5 (Hill et al., 1969). Protein concentrations were determined using the modification by Hartree (1972) of the Lowry procedure and the method according to Bradford (1976). Bovine serum albumin was used as a standard in both procedures. The partial specific volume, $\bar{v}$, for L7/L12 was determined from the amino acid composition and was found to be 0.753. Density and viscosity values for TMK_{50} buffer at 20 °C were 1.0016 g/mL and 0.009137 g/(sec·cm), respectively (D. P. Owens and K.-P. Wong, unpublished results). All water used was double distilled and deionized. Dialysis tubing was treated by boiling in 1% Na_2CO_3, 1 mM EDTA for 30 min and washed thoroughly with distilled water. All pH measurements were made with a Radiometer Model PHM64 Research pH meter equipped with a combined glass electrode (GK2303C).

Results

Purity of Protein L7/L12. Isolation as described under the Experimental Procedures yields purified L7/L12 with no detectable heterogeneity. A single band is evident from both discontinuous gel electrophoresis and sodium dodecyl sulfate–polyacrylamide gel electrophoresis, as shown in Figure 1. The latter system yields a band whose migration corresponds to a molecular weight of approximately 12 000. Sedimentation velocity schlieren patterns show that the protein moves as a single symmetric peak during its entire passage through the analytical ultracentrifuge cell. Sedimentation equilibrium experiments provide a straight line when the ln fringe displacement is plotted as a function of the square of the distance from the center of rotation. The slope of the line generated from a least-squares analysis indicates a molecular weight of 24 100 ± 200, ascertaining the dimer nature of L7/L12 in the "native" buffer (TMK_{50}).

With the possibility that protein L7/L12 generates fragments spontaneously after incubation at room temperature for 3 days or after prolonged storage at 4 °C (Liljas et al., 1978; C. A. Luer and K.-P. Wong, unpublished experiments), care was taken to assure that all measurements were performed on the intact dimer. For this reason, all the results reported here

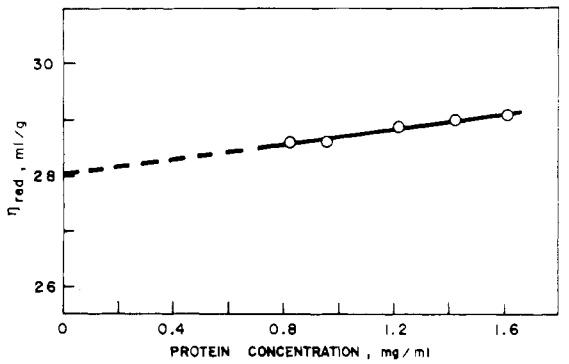

FIGURE 2: Reduced viscosities as a function of concentration for protein L7/L12. Conditions: TMK_{50} buffer, pH 7.6, 25 °C. An intrinsic viscosity of 28 ± 0.4 mL/g was obtained by extrapolation to infinite dilution.

were obtained using freshly prepared protein samples which had not been exposed to temperatures higher than 4 °C for any extended periods of time. All samples of protein L7/L12 were lyophilized and stored in a −70 °C freezer. A trace amount of tryptophan-containing contaminant has been shown to be removed after the further purification step using CM-cellulose column chromatography (C. A. Luer and K.-P. Wong, unpublished experiments).

Hydrodynamic Properties. Sedimentation velocity studies in TMK_{50} buffer yield a sedimentation coefficient of $s_{20,w}$ = 1.6 ± 0.02 S for the L7/L12 dimer. From this value the frictional coefficient is calculated to be 6.15 ± 0.15 × 10^{-8}. Comparison of this frictional coefficient with that determined for a hypothetical dry sphere of equivalent size provides a frictional coefficient ratio, f/f_{min}, of 1.84 ± 0.03.

The results of viscosity measurements of native L7/L12 are shown in Figure 2. The extrapolation of the straight line to zero protein concentration yields an intrinsic viscosity, $[\eta]$, of 28 ± 0.4 mL/g for the protein in TMK_{50} buffer. The Huggins constant, k, obtained from the slope of the straight line is 0.89 ± 0.05. The viscosity increment, or Simha parameter, is determined to be 27.6 ± 0.4, while the β factor for protein L7/L12 is computed to be 2.8 ± 0.07 × 10^6.

Spectroscopic Properties. Spectroscopic studies with L7/L12 are particularly interesting since the protein contains only two phenylalanines per monomer as the aromatic amino acids. The absence of tryptophan and tyrosine from a protein is highly unusual, although not unique (Parello & Pechere, 1971; Smith & Koffler, 1971). Since tryptophan and tyrosine absorb light to a much greater degree than does phenylalanine, spectral information about the latter in a protein is generally obscurred. The ultraviolet absorption spectrum of protein L7/L12 is shown in Figure 3a. The fine structure between 250 and 270 nm is attributed to the phenylalanines and is particularly apparent when the first derivative of the absorption spectrum is measured. The intrinsic fluorescence of phenylalanine residues in a protein environment is also rarely observed. This is due to masking by the stronger intrinsic fluorescence of tyrosine and/or tryptophan which are normally present in proteins. The fluorescence emission spectrum of protein L7/L12 is also shown in Figure 3a and clearly reflects the fine structure between 270 and 300 nm which is characteristic of phenylalanine in solution. The fluorescence emission spectrum of the protein, however, is shifted to longer wavelengths relative to the spectrum obtained for the free amino acid under the same buffer conditions (Figure 3b).

The near-UV CD spectrum of protein L7/L12 is shown in Figure 4. The spectrum reveals two negative CD bands which are expected to originate from the tertiary conformational

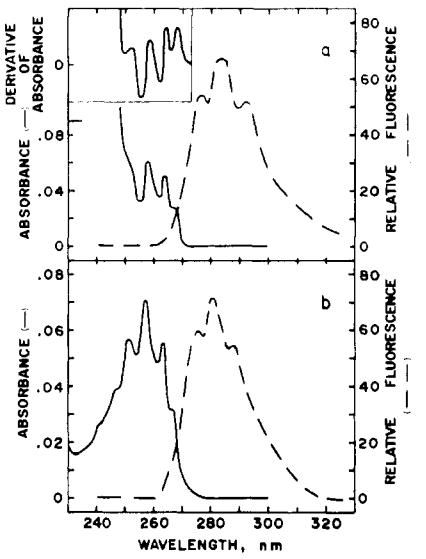

FIGURE 3: UV absorption and fluorescence spectra of protein L7/L12 and L-phenylalanine in TMK_{50} buffer at 25 °C. (a) Solid curves, the absorption spectrum and its first derivative spectrum (inset) for protein L7/L12; dashed curve, the relative fluorescence spectrum of the same protein sample. (b) Solid and dashed curves represent the absorption and relative fluorescence spectra of L-phenylalanine, respectively.

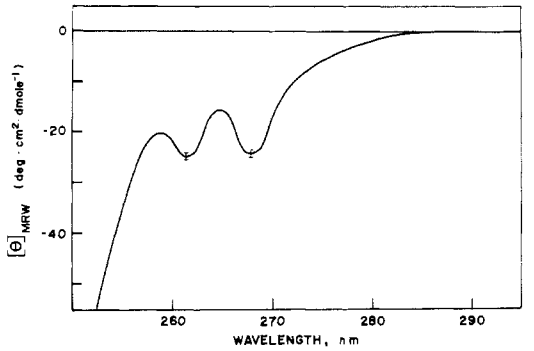

FIGURE 4: Near-UV CD spectrum of protein L7/L12. Conditions: TMK_{50} buffer, pH 7.6, 25 °C; protein concentration, 1.6 mg/mL.

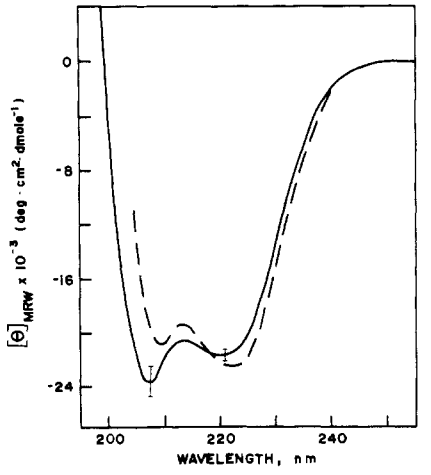

FIGURE 5: Far-UV CD spectrum of protein L7/L12. Conditions: TMK_{50} buffer, pH 7.6, 25 °C. Solid curve, experimentally obtained spectrum at a protein concentration of 50 μg/mL; dashed spectrum, theoretical spectrum generated by computer analysis according to the method of Chen et al. (1974).

environment of the phenylalanyl residues (Horwitz et al., 1969; Strickland, 1974). As was the case with the absorption and fluorescence spectra, phenylalanine CD bands are not normally observed in the near-ultraviolet due to the stronger and broader

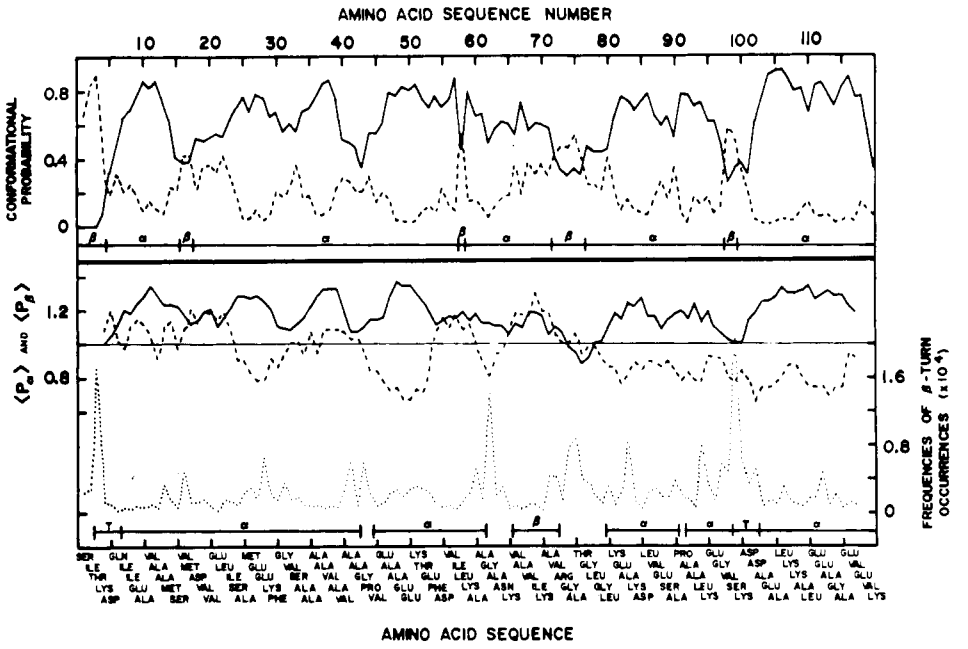

FIGURE 6: Conformational profiles of protein L7/L12 as predicted by the methods of Maxfield & Scheraga (1976) and of Chou & Fasman (1974a,b). The solid lines represent α helix, the dashed lines represent β structure, and the dotted lines represents β turns. The upper half of the figure represents the Maxfield & Scheraga plot which depicts the probability of occurrence of α helix or β structure for each residue in the amino acid sequence. The secondary structural predictions based on this computer analysis are summarized in the horizontal bars below the conformational profile. The lower half of the figure represents the Chou & Fasman predictions. In the upper portion of this representation, each point represents the average α-helical potential $\langle P_\alpha \rangle$ or β-structural potential $\langle P_\beta \rangle$ from residues $i - 3$ to $i + 3$ over the entire amino acid sequence. Regions possessing the potential to form α helices or β structures lie above the cut-off $\langle P_\alpha \rangle = \langle P_\beta \rangle = 1.0$. The lower portion of the Chou & Fasman analysis displays the β-turn profile where each point represents the product of the β-turn frequencies for residues i to $i + 3$ for each tetrapeptide in the sequence. Tetrapeptides whose probabilities exceed the β-turn cut-off of 1.6×10^{-4} are considered to possess the potential to form β turns. The secondary structural predictions according to the method of Chou & Fasman utilized updated potentials for α-helix and β-sheet structures (Fasman et al., 1976) and for β turns (Chou & Fasman, 1977) based on X-ray structural data of 29 proteins and are summarized in the horizontal bars below the conformational profile. The amino acid sequence for protein L7/L12 is represented at the bottom of the figure. The sequence is listed diagonally from left to right in groups of five amino acid residues.

CD signals of tryptophan and tyrosine present in the spectra of most proteins.

The far-UV CD spectrum is shown in Figure 5. The double trough at 208 and 222 nm and the large negative mean residue weight ellipticity values are indicative of considerable α-helical content. This assessment is substantiated by computer analysis which yields a form-fitted curve composed of ~76% α helix, ~4% β conformation, and ~20% unordered structure. The spectrum shown in Figure 5 displays larger negative mean residue ellipticity values than those spectra reported previously and is probably a function of the respective experimental conditions (Möller et al., 1970; Dzionara, 1970; Boublik et al., 1973). None of these reported spectra were obtained under "native" conditions (i.e., TMK_{50}) and with protein purified as described here.

Secondary Structure Predictions. The secondary structure of protein L7/L12 was predicted from its amino acid sequence by the methods of Chou & Fasman (1974a,b) and of Maxfield & Scheraga (1976). Both predictions agree that the amino acid sequence possesses a large potential to form α helices. The method of Chou & Fasman predicts 75% α helix, while that of Maxfield & Scheraga predicts 86%. The two methods predict small amounts of β conformation, 6% by Chou & Fasman and 11% by Maxfield & Scheraga. The secondary structure based on the methods of Chou & Fasman and of Maxfield & Scheraga are further represented in Figure 6 which graphically depicts the potential of occurrence of α helix, β conformation, and β turns over the entire sequence. In the conformational profile representing the Chou & Fasman method, each point represents the average secondary structural potential from residues $i - 3$ to $i + 3$. Over the amino-terminal half and the carboxy-terminal third of the sequence, it is apparent from the profile that α helix is potentially the dominant form of secondary structure. The method of Maxfield & Scheraga, which computes a conformational probability for each residue in the sequence, also predicts α helix in these two regions. The sequence from residues 65–79, however, does not yield the same predicted structure by the two methods. In the region where disagreement occurs, a stretch of β structure is predicted in both schemes but occurs in a slightly different location. According to the Chou & Fasman conformational profile, the potential for β conformation is extremely high for residues 66–72. No other stretch of amino acids in L7/L12 possesses a higher potential for β structure. The same sequence does, however, show a moderate probability for α helix. Residues 73–79 show no particular tendency to form either α helix or β conformation. Analysis by the method of Maxfield & Scheraga places the segment of β structure at residues 72–76. Closer examination of this computer prediction reveals that β structure in this region is only mildly dominant and that this segment of β structure could reasonably be extended in the amino-terminal direction to include residues 66–76.

A practical difference between the two predictive methods is that the potential for the existence of β turns can be easily assessed using the method of Chou & Fasman. The method of Maxfield & Scheraga does not allow for this analysis. In the β-turn profile shown in Figure 6, each point represents the product of the β-turn frequencies for residues i to $i + 3$ for each tetrapeptide in the sequence. In addition, the position of each amino acid in the β-turn tetrapeptide is taken into consideration. As demonstrated by the β-turn profile, two tetrapeptides in the sequence possess the potential to form β turns, a third lying reasonably close to the cut-off value. In

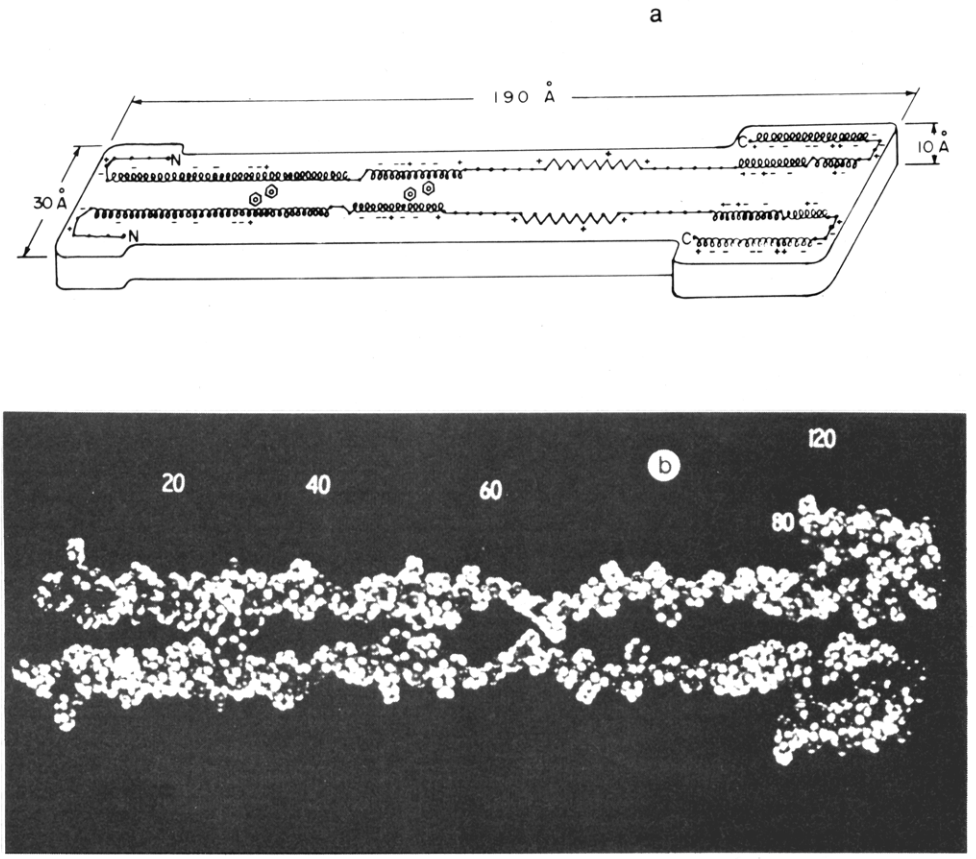

FIGURE 7: A possible molecular model of protein L7/L12. The proposed three-dimensional structure is based upon experimental data and semiempirical predictions. (a) The model is composed of 73% α helix ($\ell\ell\ell$), 6% β structure ($\Lambda\Lambda\Lambda$), 16% unordered structure (·–·–·), and 6.6% β turn (⌐¬). The positions of the charged residues and the phenylalanine side chains are indicated. The linear dimensions were approximated assuming the average rise along α-helical and β-structural axes (Dickerson & Geis, 1969). (b) Photograph of the proposed molecular model for the L7/L12 dimer constructed with Corey–Pauling–Koltun (CPK) space-filling atoms. Residues 1–59 demonstrate the essentially α-helical amino-terminal half of the molecule, whose interchain interaction is considered to play an important role in dimerization. In the photograph, this interacting region is intentionally exposed for illustrative purposes. With this artificial spatial separation, the lack of charged amino acid residues along the interacting surface and the compatibility of the interchain phenylalanine–phenylalanine ring interactions are obvious. Upon physically reducing this spatial separation in the 1–59 region, the remarkably hydrophobic faces of the monomer chains are observed to interact in the highly complementary fashion that would be expected in maintaining a stable dimer.

all three cases, the β-turn potentials for the tetrapeptides, $\langle P_t \rangle$, are greater than the corresponding potentials for both α-helix ($\langle P_\alpha \rangle$) and β-conformation ($\langle P_\beta \rangle$). Two of the tetrapeptides, residues 3–6 and 99–102, are compatible with the Maxfield & Scheraga prediction since they occur in regions where long stretches of secondary structure are disrupted. The third tetrapeptide, residues 62–65, does not conform to this observation. The conformational potentials for α helices, β conformations, and β turns as predicted for the various regions by the method of Chou & Fasman are summarized in Table I.

Rationalization of a Molecular Model. Based on the hydrodynamic and spectroscopic results presented in this report as well as the information from the two secondary structural prediction methods, a possible molecular model of protein L7/L12 is proposed and shown schematically in Figure 7a. This model also incorporates the limited structural data available from the literature. The secondary structural content of the proposed model consists of 73% α helix, 6% β structure, 16% unordered structure, and 6.6% β turns. The tentative assignment of β structure to residues 66–72 results from overlapping the prediction information from the controversial region referred to previously. This does not exclude the possibility that conformational transitions between β structure and α helix could occur in this region. Segments of α helix are proposed to exist from residues 6–42, 45–59, 80–90, 92–98, and 103–120. The disruption of long helical segments, due

Table I: Regions of α-Helix, β-Conformation, and β-Turn Tetrapeptides Predicted by the Method of Chou & Fasman (1974a,b)

	$\langle P_\alpha \rangle^a$	$\langle P_\beta \rangle^a$	$\langle P_t \rangle^a$	$\langle P_{t_2} \rangle^b$	P_t^c ($\times 10^4$)
predicted α-helix regions					
6–42	1.22	1.04			
45–61	1.26	0.92			
80–90	1.22	0.86			
92–98	1.19	0.93			
103–120	1.29	0.83			
predicted β-conformation regions					
66–72	1.18	1.3			
predicted β-turn tetrapeptides					
3–6	1.03	0.96	1.10	1.37	1.73
99–102	0.99	0.64	1.34	1.37	2.00
possible β-turn tetrapeptide					
62–65	0.96	0.80	1.20	1.10	1.41

[a] $\langle P_\alpha \rangle$, $\langle P_\beta \rangle$, and $\langle P_t \rangle$ are the average conformational potentials for the regions to be α helices, β structures, or β turns, respectively. The cut-off valve is set at 1.0. [b] $\langle P_{t_2} \rangle$ is the average conformational potential for a residue to be located in a β turn based on the second and third positions of a reverse turn. The cut-off value is set at 1.0. [c] P_t is the frequency of occurrence of a β-turn tetrapeptide. The cut-off value is 1.6×10^{-4}.

to the proline residues at positions 44 and 91, is consistent with the Chou & Fasman prediction. The termination of the essentially α helical amino-terminal half of the molecule has been assigned at residue 59 since lysine residues have been shown to prefer carboxy-terminal helical ends (Chou & Fasman, 1974a,b), and in light of the fact that a tryptic core peptide (Terhorst et al., 1972a), composed of residues 5–59 (Terhorst et al., 1973), has been obtained. The existence of this core peptide indicates that lysine-4, located in a β turn in the model, and lysine-59 are in relatively accessible regions compared with lysines-29 and -51. Tryptic cleavage at the latter two lysines, located in stable α-helical segments of the model, is achieved upon further treatment of the core peptide (Terhorst et al., 1973).

Two β turns, residues 3–6 and 99–102, are included in the proposed model. The tetrapeptide at residues 62–65, which was reasonably close to the cut-off potential, was not incorporated into the model as a β turn. Since this tetrapeptide lies in approximately the middle of the molecule, the presence or absence of a β turn at this location could be critical in the overall shape of the molecular model. The results from hydrodynamic studies indicate that L7/L12 is a highly elongated dimer. The relatively large values for the intrinsic viscosity and frictional coefficient ratio determined for protein L7/L12 suggest a highly elongated structure when compared with the corresponding values expected for globular proteins (Tanford, 1961). In addition, the values for the Huggins constant, viscosity increment and β factor calculated on the basis of the measured intrinsic viscosity are all consistent with a prolate ellipsoid of large axial ratio (Tanford, 1961). Small-angle X-ray scattering data also indicate that the L7/L12 dimer is highly elongated and suggest dimensions of 180 × 32 × 12 Å (Österberg et al., 1976). The small axis is particularly interesting since it essentially implies a flattened tertiary structure having the thickness of no more than a single α helix. This observation would provide little evidence for the existence of globular regions. By eliminating the β turn at residues 62–65, and assuming the rise along the α-helical axis per repeating unit is 1.5 Å while that for the β conformation is 3.5 Å (Dickerson & Geis, 1969), the length of the proposed monomer would be approximately 190 Å. Further analysis of the β-turn regions according to Chou & Fasman indicates that the elimination of the 62–65 tetrapeptide may not be entirely unwarranted. Comparison of $\langle P_{t_2} \rangle$ values (Table I), which are indicative of the conformational potential of a residue in a β turn based on the second and third positions of a reverse turn, demonstrates that the tetrapeptide in question does not possess nearly as great a potential as tetrapeptides 3–6 or 99–102. The fact that a tetrapeptide whose β-turn potential is near the cut-off value exists at residues 62–65 could indicate the possible location of a flexible region in the molecule.

The existence of a β turn located at residues 3–6, with its close proximity to the amino terminus, is not critical to the length or overall shape of the model. The presence or absence of a β turn in this region might become more important in the future when the mechanism of amino-terminal acetylation is better understood. The β-turn proposed to exist at residues 99–102 possesses the strongest potential for β-turn formation by all types of analysis available with the Chou & Fasman method (Table I). For this reason, this tetrapeptide is included in the proposed model as a reverse turn.

The existence of the phenylalanine CD bands in the near-ultraviolet region provides important tertiary structural information. The enhanced rotatory power of the phenylalanine CD bands suggests that the phenylalanyl residues must be located either in buried, rigid environments resulting in restricted freedom of rotation of the aromatic rings, or they must be clustered together so that their interaction can result in an induced asymmetry about the chromophores. The proposed dimer consists of two side-by-side monomer chains positioned in a parallel fashion. The term "parallel" refers to the fact that the amino termini are located at one end of the model, while the carboxy termini are at the other. With this alignment, the phenylalanine residues from adjacent monomer chains are able to interact and account for the observed near-UV CD bands. The proposed phenylalanine–phenylalanine ring interaction is analogous to the tyrosine–tyrosine interaction found to give rise to the near-ultraviolet circular dichroism of tropomyosin, a rod-like protein composed of two parallel α-helical polypeptide chains (Bullard et al., 1976). The approximate dimensions for the proposed L7/L12 dimer in solution are suggested to be 190 × 30 × 10 Å. Positioning of the monomers in an antiparallel fashion would not be consistent with interchain interaction of phenylalanine side chains since these residues are located well within the amino-terminal half of the sequence. For such an interaction to exist, there would be considerable overlap of the chains leading to a calculated length for the dimer which would far exceed that determined from small-angle X-ray scattering studies (Österberg et al., 1976). Antiparallel chains would consequently require buried phenylalanine residues in order to achieve the asymmetric environment inferred from the CD bands. The absence of any potential for the formation of a β turn between phenylalanine residues on the same chain argues against the possibility of intrachain phenylalanine clusters. The paucity of predicted β turns and the lack of globular tertiary folding inferred from the small-angle X-ray scattering studies provide little support for the existence of buried environments in the protein molecule. The intrinsic fluorescence of protein L7/L12 also argues against the phenylalanines being located in buried hydrophobic environments. If the phenylalanine residues were buried in such hydrophobic environments of globular regions, a blue shift of the fluorescence emission spectrum would be observed when comparing protein L7/L12 with free L-phenylalanine. Instead, a red shift was observed which is consistent with the interpretation that the phenylalanyl chromophores from the two chains interact with one another.

Physical construction of the proposed model using Corey–Pauling–Koltun (CPK) space-filling atomic models (Figure 7b) and Nicolson molecular models (Labquip, Reading, England) results in an interesting observation. One side of the amino-terminal helical domain (residues 6–59) is noticeably hydrophobic with all of the charged residues situated on the remaining surfaces of the helical cylinder. In fitting the monomeric chains together to construct the L7/L12 dimer, the hydrophobic faces provide an excellent surface for interaction. It is important to notice that the phenylalanine residues occur along this hydrophobic side and can interact, as proposed, in a favorable environment. Stable interchain interaction in the carboxy-terminal half of the model is not as obvious as in the amino-terminal portion. Hydrophobic interactions are possible between the β-structural (residues 66–72) and α-helical (residues 80–90 and 92–98) segments of adjacent monomer chains, but the flexibility likely in the unordered structural sequences and the lack of extended hydrophobic surfaces in the carboxy-terminal half of the model indicate that the amino-terminal portion of the molecule (corresponding to residues 1–59 in the proposed model) is

Table II: Structural Properties from Proposed Models of Ribosomal Protein L7/L12

structural property	exptl determinations	theoretical determinations: model proposed in this report	theoretical determinations: model of Gudkov et al. (1977)
dimer dimensions (A)	180 × 32 × 12[a]	190 × 30 × 10	120 × 30 × 30
frictional coefficient	6.15 ± 0.15 × 10^{-8} [b]	6.19 × 10^{-8} [c] 6.38 × 10^{-8} [e]	4.43 × 10^{-8} [d] 4.85 × 10^{-8} [e]
secondary structure			
α-helix	~76%[f]	73%	66%
β-conformation	~4	6	0
unordered structure	~20	16	34
β-turn	(not estimated)	6.6	

[a] Österberg et al. (1976). [b] Sedimentation velocity, this report. [c] Calculated according to Bloomfield et al. (1967a,b). [d] Calculated according to De La Torre & Bloomfield (1977). [e] Calculated according to Perrin (1936). [f] Computer analysis of far-ultraviolet circular dichroism spectrum, this report.

probably involved in the formation of the stable dimer.

Discussion

Supportive evidence for the suggested model comes from theoretical calculations of the frictional coefficient for the proposed structure. The treatment according to Perrin (1936) is applicable to structures approximating prolate ellipsoids with large axial ratios. Assuming long (a) and short (b) semiaxes from the model to be 95 and 15 Å, respectively, a value for the frictional coefficient of 6.38 × 10^{-8} is calculated. A prolate ellipsoid, however, does not truly reflect the essentially flattened shape of the tertiary and quaternary structure suggested by the model. The frictional coefficient obtained by the Perrin treatment might, therefore, be expected to deviate slightly from the experimentally determined coefficient. Application of the method according to Bloomfield et al. (1967a,b) does allow for a more accurate representation of the detailed shape of the model. In this procedure, the dimensions and shape of the dimer model are approximated by combining monomeric spheres of known radii. The frictional coefficient calculated by this treatment is 6.19 × 10^{-8}. The frictional coefficient obtained experimentally is 6.15 ± 0.15 × 10^{-8} and is, indeed, in excellent agreement with the theoretical frictional coefficient for the L7/L12 dimer model when calculated by the latter method. The frictional coefficient ratios (f/f_{min}) resulting from the calculated values are 1.90 from the Perrin equation and 1.85 from the Bloomfield method. These values are presented in comparison with the ratio of 1.84 determined experimentally.

Recently another possible model of the tertiary and quaternary structure for ribosomal protein L7/L12 has been proposed by Gudkov et al. (1977). This model is based upon the secondary structure predicted by Ptitsyn et al. (1973) using the method of Lim (1974a,b). Some basic similarities exist between the model proposed by Gudkov et al. and the model presented in this report. These include large amounts of α-helical structure, an elongated shape and phenylalanine tertiary environments which are compatible with some of the spectroscopic results presented here. Several important discrepancies, however, are quite apparent. The structure proposed by Gudkov et al. is represented as a dumbbell shaped dimer with the two amino-terminal halves of each monomer lying side by side in an antiparallel fashion. The carboxy-terminal halves of each monomer are folded into globular structures, each possessing a hydrophobic cavity into which the first several amino-terminal residues of the opposite monomer chain are inserted upon dimerization. Some of the structural properties of the two models are listed in Table II, where they are compared with the experimental determinations of the same parameters. The dimensions of the Gudkov model indicate a shorter and more globular structure when compared with the dimensions of the model proposed here and those measured from small-angle X-ray scattering. These differences in shape are reflected in the theoretical calculations of the frictional coefficient for the Gudkov model, which have been performed by the authors of this report for purposes of comparison. Applications of the Perrin equation and a modification of the Bloomfield treatment, which is appropriate for dumbbell shapes (De La Torre & Bloomfield, 1977), result in values which are not in very close agreement with the experimentally determined coefficient. The lack of β structure in the model proposed by Gudkov does not constitute a major discrepancy between the models since the evidence for such secondary structure in protein L7/L12 is not significant.

Another obvious difference between the two models concerns the environment of the amino termini. As mentioned previously, the Gudkov model provides for the insertion of the amino-terminal ends into hydrophobic cavities. In the model proposed in this report, the amino-terminal ends are exposed to the surrounding environment. It is of significance to note that, of the six amino-terminal acetylated proteins whose three-dimensional structures are known, all possess amino termini which are in exposed positions on the surface of the molecules (Jörnvall, 1975). While the in vivo acetylation of L12 monomers probably occurs prior to dimerization, it has been demonstrated that L12 bound to the ribosome can be acetylated at a slow but significant rate (Brot et al., 1973). If one assumes that L7/L12 exists as a dimer in the ribosome, acetylation can only take place with exposed amino termini.

The possible three-dimensional structure presented for protein L7/L12 is the result of molecular model building based upon various types of experimental data and semiempirical predictions from amino acid sequence. As further experimental findings become available, the information will be utilized to improve the existing model. In light of the fact that the crystallographic structure remains elusive, our rationalization of an approximate three-dimensional structure may be useful in the elucidation of the structure–function relationship of ribosomal protein L7/L12. The approach employed here may also be useful for other ribosomal proteins as well.

References

Bloomfield, V., Dalton, W. O., & Van Holde, K. E. (1967a) *Biopolymers 5*, 135–148.

Bloomfield, V., Van Holde, K. E., & Dalton, W. O. (1967b) *Biopolymers 5*, 149–159.

Boublik, M., Brot, N., & Weissbach, H. (1973) *Biopolymers 12*, 2083–2092.

Bradford, M. M. (1976) *Anal. Biochem. 72*, 248–253.
Brot, N., Marcel, R., Cupp, L., & Weissbach, H. (1973) *Arch. Biochem. Biophys. 155*, 475–477.
Bullard, B., Mercola, D. A., & Mommaerts, W. F. H. M. (1976) *Biochim. Biophys. Acta 434*, 90–99.
Cassim, J. Y., & Yang, J. T. (1969) *Biochemistry 8*, 1947–1951.
Chen, Y.-H., Yang, J. T., & Chau, K. H. (1974) *Biochemistry 13*, 3350–3359.
Chou, P. Y., & Fasman, G. D. (1974a) *Biochemistry 13*, 211–222.
Chou, P. Y., & Fasman, G. D. (1974b) *Biochemistry 13*, 222–245.
Chou, P. Y., & Fasman, G. D. (1977) *J. Mol. Biol. 115*, 135–175.
Davis, B. J. (1964) *Ann. N.Y. Acad. Sci. 121*, 404–427.
De La Torre, J. G., & Bloomfield, V. (1977) *Biopolymers 16*, 1747–1763.
Dickerson, R. E., & Geis, I. (1969) in *The Structure and Action of Proteins*, p 32, W. A. Benjamin, Menlo Park, CA.
Dzionara, M. (1970) *FEBS Lett. 8*, 197–200.
Fasman, G. D., Chou, P. Y., & Adler, A. J. (1976) *Biophys. J. 16*, 1201–1238.
Gudkov, A. T., Behlke, J., Vtiurin, N. N., & Lim, V. I. (1977) *FEBS Lett. 82*, 125–129.
Hamel, E., Koka, M., & Nakamoto, T. (1972) *J. Biol. Chem. 247*, 805–814.
Hartree, E. F. (1972) *Anal. Biochem. 48*, 422–427.
Hill, W. E., Rossetti, G. P., & Van Holde, K. E. (1969) *J. Mol. Biol. 44*, 263–277.
Horwitz, J., Strickland, E. H., & Billups, C. (1969) *J. Am. Chem. Soc. 91*, 184–190.
Huggins, M. L. (1972) *J Am. Chem. Soc. 64*, 2716–2718.
Jörnvall, H. (1975) *J. Theor. Biol. 55*, 1–12.
Liljas, A., & Kurland, C. G. (1976) *FEBS Lett. 71*, 130–132.
Liljas, A., Eriksson, S., Donner, D., & Kurland, C. G. (1978) *FEBS Lett. 88*, 300–304.
Lim, V. I. (1974a) *J. Mol. Biol. 88*, 857–872.
Lim, V. I. (1974b) *J. Mol. Biol. 88*, 873–894.
Maxfield, F. R., & Scheraga, H. A. (1976) *Biochemistry 15*, 5138–5153.
Möller, W. (1974) in *Ribosomes* (Tissieres, A., Nomura, M., & Lengyel, P., Eds.) pp 711–731, Cold Spring Harbor Press, Cold Spring Harbor, NY.
Möller, W., Castleman, H., & Terhorst, C. P. (1970) *FEBS Lett. 8*, 192–196.
Möller, W., Groene, A., Terhorst, C., & Amons, R. (1972) *Eur. J. Biochem. 25*, 5–12.
Österberg, R., Sjöberg, B., Liljas, A., & Pettersson, I. (1976) *FEBS Lett. 66*, 48–51.
Parello, J., & Pechere, J.-F. (1971) *Biochimie 53*, 1079–1083.
Perrin, F. (1936) *J. Phys. Radium 7*, 1–11.
Ptitsyn, O. B., Denesyuk, A. I., Finkelstein, A. V., & Lim, V. I. (1973) *FEBS Lett. 34*, 55–57.
Scheraga, H. A., & Mandelkern, L. (1953) *J. Am. Chem. Soc. 75*, 179–184.
Simha, R. (1940) *J. Phys. Chem. 44*, 25–34.
Smith, R. W., & Koffler, H. (1971) *Adv. Microb. Physiol. 6*, 219–339.
Strickland, E. H. (1974) *CRC Crit. Rev. Biochem.* 3, 113–175.
Tanford, C. (1961) in *Physical Chemistry* of *Macromolecules*, pp 317–456, Wiley, New York.
Terhorst, C., Möller, W., Laursen, R. & Wittman-Liebold, B. (1972a) *FEBS Lett. 28*, 325–328.
Terhorst, C. P., Wittmann-Liebold, B., & Möler, W. (1972b) *Eur. J. Biochem. 25*, 13–19.
Terhorst, C., Möller, W., Laursen, R., & Wittmann-Liebold, B. (1973) *Eur. J. Biochem. 34*, 138–152.
Traub, P., Mizushima, S., Lowry, C. V., & Nomura, M. (1971) *Methods Enzymol. 20*, 391–407.
Weber, K., & Osborn, M. (1969) *J. Biol. Chem. 244*, 4406–4412.
Wittmann-Liebold, B., Robinson, S. M. L., & Dzionara, M. (1977) *FEBS Lett. 81*, 204–213.
Wong, K.-P., & Paradies, H. H. (1974) *Biochem. Biophys. Res. Commun. 61*, 178–184.